

# RADIATION SOURCES AT SIBERIA-2 STORAGE RING

V.N. Korchuganov, N.V. Smolyakov, N.Yu. Svechnikov, S.I. Tomlin,  
RRC Kurchatov Institute, Moscow 123182, Russia

## Abstract

In this report, two projects of radiation sources at Siberia-2 storage ring are considered. The first one is in-vacuum short period mini-undulator, which is intended for generation of bright X-ray beams. It is shown the feasibility of diffraction-limited in vertical direction X-ray source, which is to say that vertical emittance of the electron beam is equal to diffraction emittance of generated by undulator 2 KeV photon beam.

The second source will utilize edge radiation, which is generated in the fringe fields of the bending magnets. Numerical simulations show that the edge radiation is more intensive in infrared – ultraviolet spectral range as compared with standard synchrotron radiation (SR) from regular part of the same bending magnet.

## INTRODUCTION

The magnetic system of Siberia-2 storage ring (electron beam energy of 2.5 GeV) consists of six mirror-symmetrical cells, each containing an achromatic bend and a gap with a zero dispersion function, see Fig.1 [1, 2]. The distance between the down- and upstream edges of the bending magnets is 5340 mm. The portion of straight section, suitable for insertion device loading, is about 3 m in length. The Siberia-2 lattice is so designed that the different requirements for wigglers and undulators are satisfied. So, the straight sections with small values of betatron functions, where electron beam has minimum sizes, provide optimum performance for wigglers, while the straight sections with large betatron functions, where the electron beam has small angular divergences, are optimum for undulators.

Now at Siberia-2 storage ring SR is mainly in use. Its flux is of the order of  $10^{11}$ - $10^{13}$  phot/s/mrad/(BW=0.1%) in 4 – 40 KeV spectral range. One superconducting wiggler with 7.5 T magnetic field amplitude is also installed. At the same time nearly all straight sections are planned to complete with different insertion devices in the nearest future, see Fig.1 and Table 1.

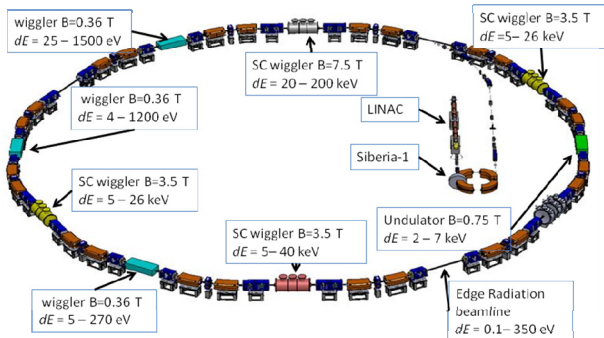


Fig.1 Siberia-2 layout with projected insertion devices.

#smolyakovnv@mail.ru

Table 1. Main parameters of insertion devices

	$B_{max}$ T	$\lambda_u$ , mm	Number of periods	Spectral range KeV
s/c wiggler	7.5	164	10	20-200
s/c wiggler	3	44	35	5-40
wiggler	0.36	80	51	5.5-270 eV
undulator	0.75	7	300	2-7
edge radiation	-	-	-	0.1-350 eV

## UNDULATOR RADIATION

The most important feature of undulator radiation beam is its brilliance, which is mainly determined by the electron beam emittances and radiation diffraction phase volume, which is equal to  $\lambda/4\pi$ , where  $\lambda$  is radiation wavelength. A light source is called diffraction - limited if the electron beam emittance is smaller than that of the photon beam.

Nowadays a natural horizontal emittance of electron beam in Siberia-2 at 2.5 GeV is equal to 98 nm-rad [1]. Operating parameters of storage ring are listed in the Table 2. In addition to existing optical lattice new more brilliant lattice with horizontal emittance 18 nm-rad (at 2.5 GeV energy) has been developed (Table 2), The new lattice allows to obtain the horizontal emittance of 4.9 nm-rad at 1.3 GeV. Vertical emittance of electron beam is 49 pm-rad with a coupling factor of betatron oscillation  $k \approx 0.01$  for Siberia-2. Thus, vertical emittance is equal to emittance of 2 keV photons. It is important to note that the new brilliant lattice can be obtained by changing of currents in lattice magnetic elements only.

Table 2: Siberia-2 Storage Ring Parameters

Lattice	“standard”	“brilliance”
Energy	2.5 GeV	1.3 GeV
Emittance	98 nm-rad	4.9 nm-rad
Beam size: $\sigma_x/\sigma_y$	1500/78	363/17
Circumference	124.128 m	
Coupling	0.01	
Momentum compaction	0.0103	$4.2 \times 10^{-3}$
Betatron tunes: $Q_x/Q_y$	7.775/6.695	9.707/5.622
R.m.s. energy spread	$9.5 \times 10^{-4}$	$5 \times 10^{-4}$
Damping times: $\tau_x, \tau_y, \tau_s$	3.2; 3; 1.5 ms	22; 22; 11 ms
Beam current	100-300 mA	

For generation of 2 KeV photons by 1.3 GeV electron beam, undulator should match rigid requirements, see Table 3. Undulator has very short 7 mm period and high peak field 0.75 T. Last years technology for undulators was greatly advanced [3, 4, 5]. It gives us a hope that production of the undulator with such record parameters will be possible.

Table 3: Main parameters of the undulator.

Gap	2.2 mm
Permanent magnet material	NdFeB
Residual field, $\mu_0 H_c$	1.2 T
Undulator period, $\lambda_u$	7 mm
Poles width, $w$	50 mm
Field amplitude, $B_0$	0.75 T
Undulator parameter, $K$	0.492
Number of periods	300
Undulator length, $L_{UD}$	2.1 m
Wavelength of fundamental, $\lambda_1$	6.06 Å
Photon energy of fundamental, $\epsilon_1$	2.045 KeV

A set of computer codes SMELRAD [6] has been used for undulator radiation simulation. Flux density distributions of fundamental harmonic in horizontal and vertical directions are shown in Fig. 2. Three cases were considered: 1) electron beam with zero horizontal and vertical emittances:  $\epsilon_x = \epsilon_z = 0$ ; 2)  $\epsilon_x = 4.9$  nm·rad,  $\epsilon_z = 49$  pm·rad; 3)  $\epsilon_x = 4.9$  nm·rad,  $\epsilon_z = 4.9$  pm·rad. One can see that electron beam emittance essentially influence on radiation angular distribution. At the same time a tenfold decrease of electron beam emittance in vertical direction from  $\epsilon_z = 49$  pm·rad to  $\epsilon_z = 4.9$  pm·rad does not change notably the radiation distributions. Thus we can conclude that in vertical plane the diffraction limit is achieved.

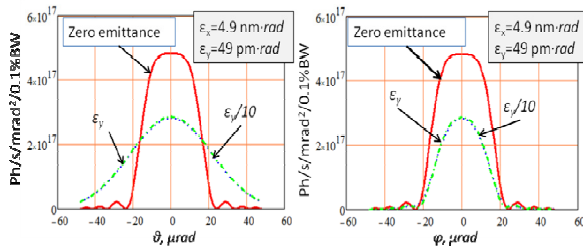


Fig.2. Horizontal (left) and vertical (right) angular distribution of fundamental harmonic.

## EDGE RADIATION

The pole of each bending magnet is divided into two parts: the long one with the main field  $B = 1.7$  T (bending radii of 490.54 cm) and a shorter one with a

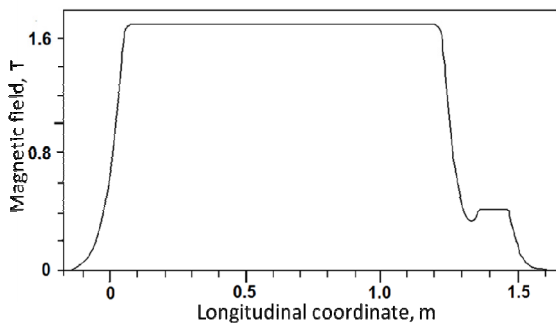


Fig.3. Magnetic field of Siberia-2 bending magnet

quarter field  $B/4 = 0.425$  T. The shorter part of the magnetic pole with quarter field adjoins to the long straight section. The measured field of the bending magnets is shown in Fig. 3.

Electromagnetic edge radiation (ER) is produced by a relativistic charged particle in its passage through the fringe fields at the bending magnet edges. In long-wavelength spectral range (at radiation wavelengths much longer than synchrotron radiation critical wavelength) its intensity is much higher than corresponding intensity of synchrotron radiation from uniform magnetic field of the same bending magnet [7, 8, 9]. Measurements of long-wave ER [10, 11] strengthened the belief that electron beam ER can be used as a bright source of electromagnetic radiation in the infrared - vacuum ultraviolet spectral range. Several infrared beam lines utilizing ER are now in operation [12, 13, 14].

The photons emitted at two adjacent bending magnets bounding a straight section, appear in the same narrow cone and are subsequently synchronized by the electron itself. This leads to the interference of ER. The interference manifests itself as additional oscillations in the radiation intensity distribution [15, 16, 17].

The distance between the down- and upstream edges of the bending magnets is 5340 mm. Synchrotron radiation with 7.2 keV critical energy from the homogeneous 1.7 T field is extracted by  $10 \times 10$  mrad<sup>2</sup> beam lines. The radiation distributions were calculated at the following beam parameters [1]: 100 mA beam current,  $\sigma_x = 0.72$

mm,  $\sigma_x' = 0.11$  mrad,  $\sigma_z = 0.014$  mm,  $\sigma_z' = 0.056$  mrad. Since 0° port has a mask with entrance aperture 44 mm hor.  $\times$  16 mm vert. which is installed at 1580 mm downstream from the straight section, ER distributions were calculated in the plane of this mask. The numerical evaluations are carried out with the package of computer codes SMELRAD (SiMulation of ELectromagnetic RADIation) [6]. Simulations include so-called “velocity term” and near-field effects. The program computes step by step the electron’s trajectory in the given magnetic field, which should be prescribed in the input file with the magnetic field data. It makes possible to use experimentally measured data. Electron beam emittance effects are calculated via numerical convolution.

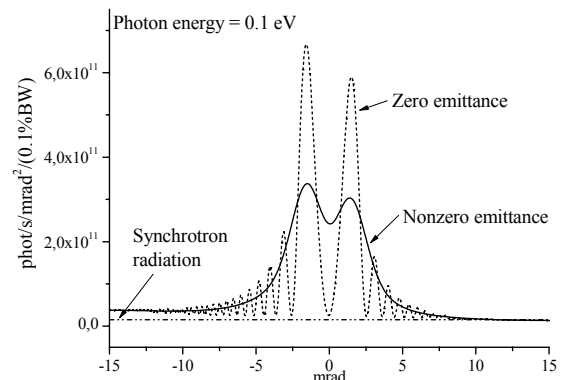


Fig. 4. Horizontal distributions of ER in the median plane.

Figure 4 displays the computed flux density in the Siberia-2 electron orbit plane 1580 mm downstream of a straight section. The flux density with 0.1 eV photon energy is plotted versus horizontal angle. The calculations were carried out for the electron beam with zero and nonzero electron beam emittance. One can readily see that the nonzero emittance effects smooth out the fine interference oscillations. The distributions are substantially asymmetric about the straight section axis because of the relatively short distance from the screen to the straight section. The radiation distribution tends to the correspondent SR intensity as the distance from the straight section axis in the median plane increases.

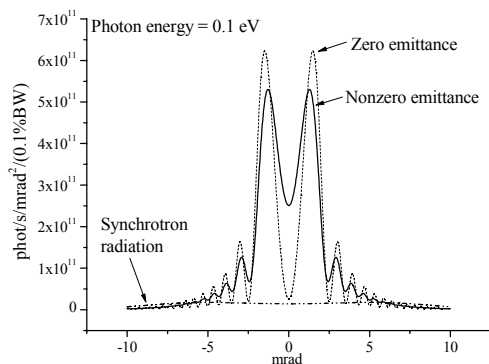


Fig. 5. Vertical distributions of edge radiation.

The vertical cross sections of 0.1 eV ER distributions along straight section axis (with zero horizontal angle) is shown in Fig. 5. For comparison the correspondent distribution of synchrotron radiation from 1.7 T bending field is also plotted in the same figure. It is easy to see from Figs. 4 and 5 that ER is much brighter than synchrotron radiation in long wavelength spectral range.

In Fig. 6, the ER and synchrotron radiation fluxes into  $10 \times 10$  mrad<sup>2</sup> solid angle centered on the straight section axis are shown. From this figure we notice that for a given aperture the flux of edge radiation far exceeds the synchrotron radiation flux for the photon energies less than 350 eV.

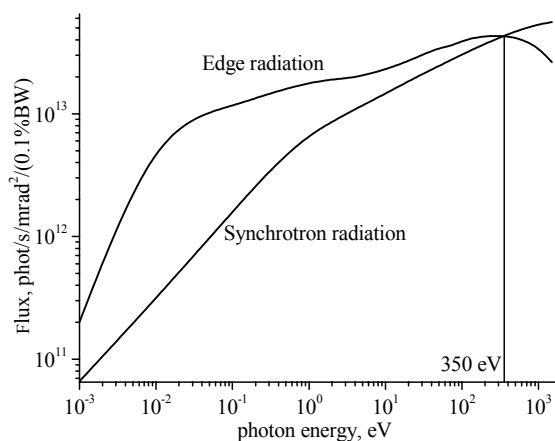


Fig. 6. ER and SR fluxes into  $10 \times 10$  mrad<sup>2</sup> solid angle.

It is worthy of note that application of ER considerably reduces thermal and radioactive load on beam line elements. Indeed, the generation of hard X-rays is suppressed along the straight section because the magnetic field is depressed at fringe regions. The total power generated in 1.7 Tesla bending field by the 100 mA electron beam into  $10 \times 10$  mrad<sup>2</sup> solid angle is equal to 113 W. At the same time the total power generated by this electron beam along straight section axis into  $28 \times 10$  mrad<sup>2</sup> (entrance aperture of mask) is equal to 18 W only.

## REFERENCES

- [1] V.V. Anashin, A.G. Valentinov, V.G. Veshcherevich et al., Nucl. Instr. and Meth. **A282** (1989) 369.
- [2] Korchuganov V., Blokhov M., Kovalchuk M. et al., Nucl. Instr. Meth. **A543** (2005) 14.
- [3] Rakowsky G., Aspenleiter J.J., Graves W.S. et al. Proceedings of 1997 Particle Accelerator Conference. 1997. V. 3. P. 3497.
- [4] Sasaki S. Proceedings of 2005 Particle Accelerator Conference. 2005. P. 982.
- [5] Kim D.E., Park K.H., Oh J.S. et al. Proceedings of 2007 Asian Particle Accelerator Conference. 2007. P. 190.
- [6] Smolyakov N.V. Nucl. Instr. and Meth. **A467-468** (2001) 210.
- [7] E.G. Bessonov, Sov. Phys. JETP **53** (1981) 433.
- [8] O.V. Chubar, N.V. Smolyakov, J. Optics (Paris) **24**, No. 3 (1993) 117.
- [9] O.V. Chubar, N.V. Smolyakov, Proc. of the 1993 IEEE PAC Conf., Washington (1993) 1626.
- [10] Shirasawa K., Smolyakov N.V., Hiraya A., Muneyoshi T. Nucl. Instr. and Meth. **B199** (2003) 526.
- [11] Smolyakov N.V., Hiraya A. Nucl. Instr. and Meth. **A543** (2005) 51.
- [12] Y.-L. Mathis, P. Roy, B. Tremblay et al., Phys. Rev. Letters **80** (1998) 1220.
- [13] T.E. May, R.A. Bosch and R.L. Julian, Proc. of the 1999 PAC Conf., New York (1999) 2394.
- [14] R.A. Bosch, R.L. Julian, R.W.C. Hansen et al., Proc. of the 2003 PAC Conf., Portland (2003) 929.
- [15] M.M. Nikitin, A.F. Medvedyev, M.B. Moiseev, Sov. Tech. Phys. Lett. **5** (1979) 347.
- [16] M.M. Nikitin, A.F. Medvedyev, M.B. Moiseev, V.Ya. Epp, Sov. Phys. JETP **52** (1980) 388.
- [17] M.M. Nikitin, A.F. Medvedyev, M.B. Moiseev, IEEE Trans. Nucl. Sci. **NS-28** (1981) 3130.